Bright far-red fluorescent protein for whole-body imaging

Dmitry Shcherbo[1,3], Ekaterina M Merzlyak[2,3], Tatiana V Chepurnykh[2], Arkady F Fradkov[1], Galina V Ermakova[1], Elena A Solovieva[1], Konstantin A Lukyanov[1], Ekaterina A Bogdanova[1], Andrey G Zaraisky[1], Sergey Lukyanov[1] & Dmitriy M Chudakov[1]

For deep imaging of animal tissues, the optical window favorable for light penetration is in near-infrared wavelengths, which requires proteins with emission spectra in the far-red wavelengths. Here we report a far-red fluorescent protein, named Katushka, which is seven- to tenfold brighter compared to the spectrally close HcRed or mPlum, and is characterized by fast maturation as well as a high pH-stability and photostability. These unique characteristics make Katushka the protein of choice for visualization in living tissues. We demonstrate superiority of Katushka for whole-body imaging by direct comparison with other red and far-red fluorescent proteins. We also describe a monomeric version of Katushka, named mKate, which is characterized by high brightness and photostability, and should be an excellent fluorescent label for protein tagging in the far-red part of the spectrum.

Homologs of the green fluorescent protein from *Aequoria victoria* (avGFP) are widely used in biotechnology as well as fundamental and applied science, with the range of their applications being ever extended[1–3]. In particular, fluorescent proteins provide unique opportunities for noninvasive labeling and tracking of specific cell types in living organisms in real time. Together with the development of new systems for whole-body imaging, fluorescent proteins allow visualization of changes in target-gene promoter activity, tracking cellular movement in embryogenesis and inflammatory processes, monitoring migration of small parasites within a host, and studying important aspects of cancer, such as tumor cell trafficking, invasion, metastasis and angiogenesis[3–7]. Furthermore, photoactivatable fluorescent proteins[7–10] and fluorescent Timers[11,12] expand the scope of temporally and spatially controlled tracking experiments.

The main photon absorbers within the visual spectrum in animal tissues are melanin and hemoglobin. Wavelengths longer than 1,100 nm are absorbed by water. Additionally, light-scattering intensity drops off as the wavelength increases. For these reasons the favorable 'optical window' for the visualization in living tissues is approximately 650–1,100 nm (ref. 13; **Fig. 1a**). Recently far-red fluorescent proteins whose emission maxima reach the 650-nm barrier have been developed, such as HcRed[14], mPlum[15] and AQ143 (ref. 16). But the available red and far-red fluorescent proteins are either characterized by deficient brightness (approximately 10% of that of EGFP) or their emission peaks are too short-wave to reach the optical window (**Table 1**). Besides, excitation maxima of most bright red fluorescent proteins are around 550–560 nm, wavelengths at which living tissues are almost opaque (**Table 1** and **Fig. 1a**) and fluorescence of these proteins cannot be effectively excited. Therefore, there is a pressing need for the development of bright far-red fluorescent proteins that should minimize light loss and substantially raise sensitivity of the whole-body imaging techniques.

Here we report Katushka, a fluorescent protein that is characterized both by high brightness and far-red fluorescence. Direct comparison with existing red and far-red fluorescent proteins demonstrated that Katushka is strongly preferable for visualization within living tissues. We also generated a monomeric version of Katushka, named mKate. Owing to the high brightness, far-red fluorescence and high photostability, mKate is a protein of choice for monitoring fused proteins in a whole organism, and also for combining with other fluorescent proteins in multicolor labeling and FRET techniques.

RESULTS

Development of the far-red fluorescent protein

Recently we had cloned a bright red fluorescent protein from the sea anemone *Entacmaea quadricolor,* named eqFP578, and had developed an enhanced version of this protein, TurboRFP[17]. Owing to fast maturation, high pH-stability and high brightness (the calculated brightness is ~1.7-fold higher than that of DsRed2), TurboRFP presented a favorable starting point for the generation of a bright far-red fluorescent protein.

To look for further red-shifted variants, we used a combination of site-specific and random mutagenesis. Available crystal structures of the related eqFP611 (refs. 18,19) revealed which of the amino acids surrounding the chromophore of TurboRFP were the most interesting to modify. We generated three libraries using a mixture of TurboRFP and several of its precursors as the initial

[1]Shemiakin-Ovchinnikov Institute of Bioorganic Chemistry, Miklukho-Maklaya 16/10, 117997 Moscow, Russia. [2]Evrogen JSC, Miklukho-Maklaya 16/10, Moscow 117997, Russia. [3]These authors contributed equally to this work. Correspondence should be addressed to D.M.C. (chudakovdm@mail.ru).

RECEIVED 20 JUNE; ACCEPTED 30 JULY; PUBLISHED ONLINE 26 AUGUST 2007; DOI:10.1038/NMETH1083

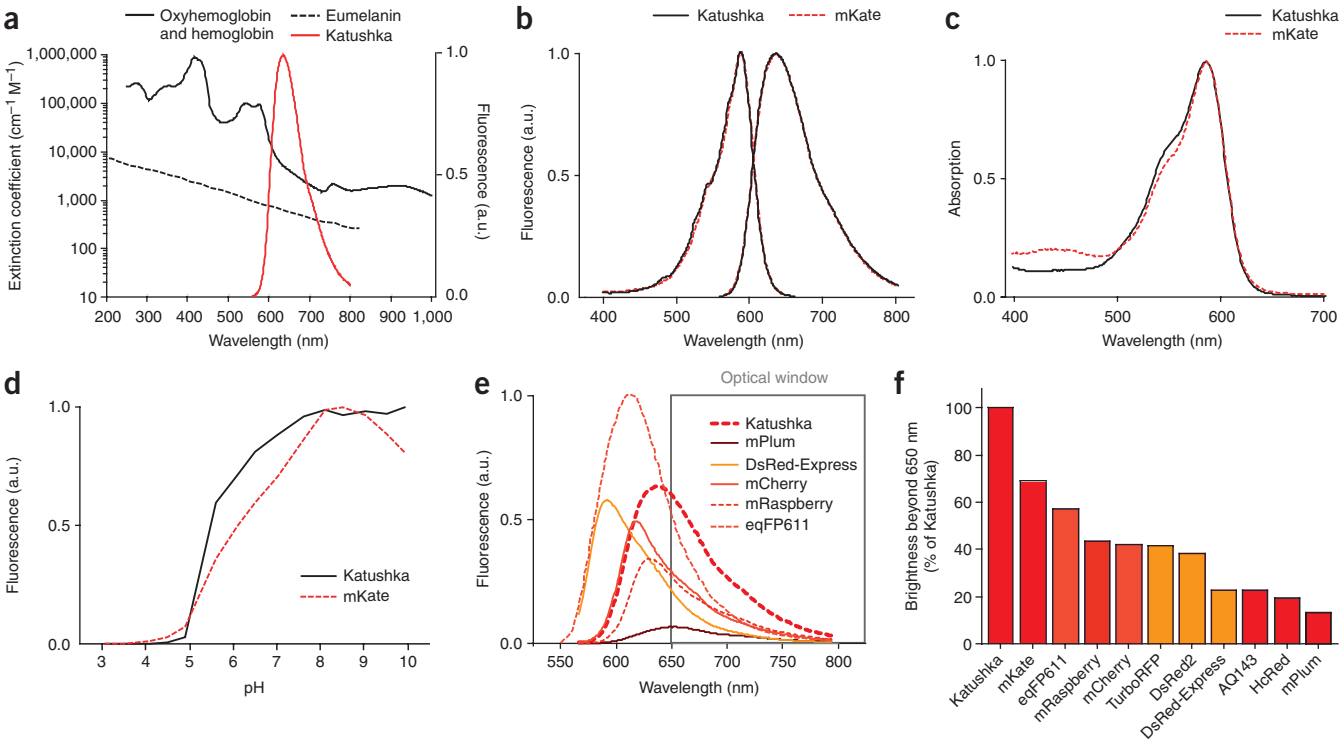

Figure 1 | Spectral characteristics. (**a**) Absorption spectra of major intracellular absorbers and Katushka. Exctinction coefficients of oxyhemoglobin and hemoglobin were averaged. Data are from http://omlc.ogi.edu. (**b**) Fluorescence excitation and emission spectra of Katushka and mKate. (**c**) Absorption spectra of Katushka and mKate. (**d**) pH stability of Katushka and mKate fluorescence. (**e**) Emission spectra of selected fluorescent proteins given proportionally to their calculated brightness. (**f**) Fluorescence brightness of compared fluorescent proteins within the optical window, calculated as definite integrals over wavelength limits from 650 to 800 nm.

template. Using degenerate primers, we created three libraries encoding protein variants with different possible amino acids containing small, bulky or polar side chains at position 148 (Gly, Ala, Thr, Cys, Ser or Phe, Leu, Ile, Met, Val or Asn, Lys, Asp, Glu, Gln, His, Tyr) in combination with different possible amino acids at position 165 (Gly, Ala, Thr, Cys, Ser) and 181 (Phe, Leu, Ile, Met, Val) (numbering is in accordance with avGFP alignment; **Supplementary Fig. 1** online). In total, each of the first two libraries contained 125 variants and the third contained 175 variants of the amino acids surrounding the chromophore. Then we randomly mutagenized each library (**Supplementary Methods** online) and cloned them into the expression vector pQE30 (Qiagen) and expressed it in *E. coli* XL1 Blue strain (Invitrogen). We screened ~100,000 individual clones for variants characterized by high brightness in the far-red part of the spectrum using a fluorescent stereomicroscope Olympus SZX-12 equipped with the appropriate

Table 1 | Spectral characteristics of selected red and far-red fluorescent proteins

Protein	Excitation maximum	Emission maximum	QY	EC ($M^{-1}cm^{-1}$) (at excitation maximum)	Relative brightness[a]	Brightness beyond 650 nm[b]	References
TurboRFP	553	574	0.67	92,000	1.87	42	17
TagRFP	555	584	0.48	100,000	1.46	34	17
DsRed2	563	588	0.55	43,800[c] 65,000[d]	0.73[c] 1.08[d]	38	26,27
DsRed-Express	555	588	0.51	38,000[c] 39,500[d]	0.59 0.61[d]	23	28
eqFP611	559	611	0.45	78,000	1.06	57	29
mCherry	587	615	0.22	72,000[c] 78,000[d]	0.48[c] 0.52[d]	42	24
mRaspberry	598	625	0.15	86,000[c] 79,000[d]	0.39[c] 0.36[d]	44	15
Katushka	588	635	0.34	65,000	0.67	100	
mKate	588	635	0.33	45,000	0.45	67	
mPlum	590	649	0.10	41,000[c] 22,000[d]	0.12[c] 0.07[d]	13	15
HcRed	594	649	0.05	70,000	0.10	20	14
AQ143	595	655	0.04	90,000	0.11	23	16

[a]Brightness is calculated as a product of molar extinction coefficient and a fluorescence quantum yield and is given comparing to the brightness of EGFP. [b]Calculated as definite integrals over wavelength limits from 650 to 800 nm, % of Katushka. [c]Published data. [d]Our data.
QY, quantum yield; EC, extinction coefficient.

filter set (excitation filter 520–620 nm, emission filter 650LP). For the selected *E. coli* colonies we measured the emission spectra using a spectrophotometer SMS 2 VIS built into the stereomicroscope.

At this step, we found a red-shifted variant that had a fluorescence emission peak at 635 nm. This variant contained Ser148, wild-type Ser165, Leu181 as well as random substitutions H199Y and H203R. Notably, position 203 is in close proximity to the chromophore and the bulky arginine should greatly affect the fluorescent properties of the resulting protein.

We optimized this variant by random mutagenesis. We screened random libraries for the clones characterized by fast maturation at 37 °C and a bright fluorescence in the far-red region of the spectrum. For the next cycle, we selected only the clones that preserved the far-red emission maximum. We performed a total of 4 cycles of random mutagenesis, yielding the final version of the protein, named Katushka (see **Supplementary Fig. 1** for the protein sequence).

Characterization of Katushka *in vitro*

Excitation and emission spectra of Katushka peak at 588 nm and 635 nm, respectively (**Fig. 1b**). The emission peak is located in the favorable part of the spectrum, entering the 'tissue optical window' beyond the absorbance of hemoglobin and melanin (**Fig. 1a**). At the same time, its excitation peak is located close to the maximal excitation wavelength reported for all fluorescent proteins, permitting effective excitation in living tissues (**Table 1**).

Katushka is characterized by fast maturation at 37 °C with a half-time of 20 min, which is superior to the fast-maturing mCherry (half-time of 40 min; maturation measured according to ref. 17). Maturation of the red chromophore is complete, as the absorbance spectrum of a freshly purified Katushka protein represents a single narrow peak (**Fig. 1c**). Fluorescence of Katushka is pH-stable, with a pK_a of 5.5 (**Fig. 1d**). The fluorescence quantum yield and extinction coefficient for Katushka are 0.34 and 65,000 M^{-1} cm^{-1} respectively, resulting in a calculated brightness of 0.67 of EGFP. This is higher than that of any other fluorescent proteins with an emission maximum beyond 620 nm (**Table 1**). Within the 650–800 nm optical window, Katushka is essentially brighter than any known red or far-red fluorescent protein (**Fig. 1e,f**). Direct comparison with various red and far-red fluorescent proteins in living bacterial cells showed superior brightness of Katushka in the far-red part of the spectrum (**Supplementary Fig. 2** online).

Characterization of Katushka in living cells

We transiently transfected HeLa and Phoenix Eco cells with vectors driving expression of selected red fluorescent proteins. The Phoenix Eco cell line provides high expression from vectors with an SV40 origin of replication and allows testing of fluorescent protein behavior in cells at high concentration. In our experience, proteins that have a tendency to aggregate, and are therefore nonoptimal for the generation of stable cell lines and transgenic animals, commonly demonstrate aggregation or abnormal localization effects in Phoenix Eco cells within several days.

Cells transfected with Katushka had bright far-red fluorescence 10–14 h after transfection, indicating fast protein maturation. Cells expressing DsRed2 and DsRed-Express showed abnormal Golgi-like localization 5–7 d after transfection, and those expressing mCherry and mRaspberry had dot-like aggregates. Cells expressing Katushka contained no visible aggregates or nonspecific localization at the same time point, indicating that it should be highly suitable for the generation of stable cell lines and transgenic animals (**Supplementary Fig. 3** online).

Comparison in *Xenopus laevis*

To test Katushka for the visualization of cells inside a multicellular organism, we compared it with one of the most widely used red fluorescent proteins, DsRed-Express, and the far-red fluorescent protein mPlum. We expressed each fluorescent protein in muscle cells of *X. laevis* embryos. To target the expression of the fluorescent proteins to these cells, we used the 800-bp fragment of the *X. laevis* cardiac actin promoter, which can specifically drive reporter expression in cardiac and skeletal muscle cells derived from the embryonic somites[20]. In the case of Katushka transgenics, we observed red fluorescence both in the somites and in the heart rudiment starting from stages 32–33 (ref. 21; **Fig. 2a–d** and **Supplementary Fig. 4** online). *X. laevis* expressing DsRed-Express displayed bright red fluorescence in the somites, but little signal could be detected in the heart at stages 32–33 (**Fig. 2e–h** and **Supplementary Fig. 4**).

Assuming that heart rudiment at stages 32–33 is still surrounded by vegetal yolk-enriched cells, this difference between transgenics could be explained by longer-wavelength emission of Katushka, which has an advantage in tissue penetration. Somite cells are

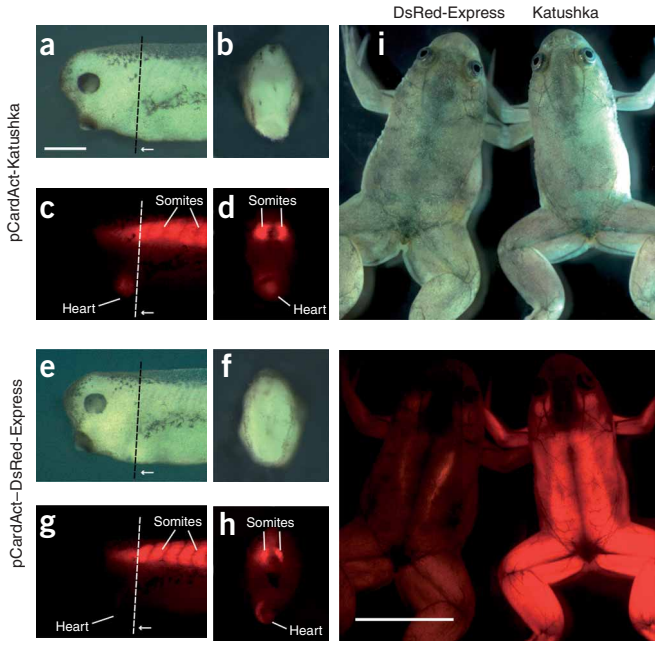

Figure 2 | Comparison in *X. laevis* embryos. (**a–h**) Transgenic *X. laevis* embryos expressing Katushka (**a–d**) or DsRed-Express (**e–h**) under the control of cardiac actin promoter. White light (**a**,**b** and **e**,**f**) and fluorescence (rhodamine filter set; **c**,**d** and **g**,**h**) images of the anterior part of the transgenic embryos, stage 33, left side, dorsal side to the top (**a**,**c**,**e**,**g**) or head part of the corresponding embryo (**b**,**d**,**f**,**h**) imaged from the planes of cut indicated by dotted lines (direction of the view is indicated by arrows). (**i**) White-light (top) and fluorescence (bottom) image of 2.5-month-old frogs expressing DsRed-Express (left) or Katushka (right) from the dorsal side. Scale bars, 0.5 mm (**a–h**) and 10 mm (**i**).

equally visible in both Katushka and DsRed-Express transgenics because they are only covered by the thin and transparent dorsal epidermis, which is largely free of yolk. Also, the expression of the fluorescent protein reporters driven by cardiac actin promoter is substantially higher at stages 32–33 in somite cells when compared with that in the heart. To verify this supposition, we cut transgenic embryos transversely just behind their hearts. When inspected from the cut surface, both Katushka and DsRed-Express transgenics displayed similar levels of red fluorescence (**Fig. 2d**,**h**). We performed analogous experiments with mPlum, which is characterized by even longer emission wavelength than Katushka but a tenfold weaker fluorescence. mPlum could be hardly detected in heart rudiments, testifying to the importance of brightness in addition to emission wavelength as being an important determinant in the utility of fluorescent protein *in vivo* (**Supplementary Fig. 4**). Remarkably, after 2.5 months, Katushka was visible in the whole body of *X. laevis* using a Leica MZFLIII fluorescent stereomicroscope (excitation filter 546/10; emission filter 565LP), whereas DsRed-Express could be hardly visualized (**Fig. 2i**).

Notably, tadpoles bearing the Katushka transgenic construct demonstrated higher viability in comparison with those bearing DsRed-Express vector. Of the Katushka-expressing transgenic tadpoles selected at stage 46 (5 d), 38% reached stage 60 (50 d) (18 tadpoles from 48 selected ones). In contrast, only 20% of DsRed-Express–expressing transgenic tadpoles, selected at stage 46, were still alive by stage 60 (9/45 tadpoles). The relatively low death rate of Katushka transgenic tadpoles is comparable to the viability of transgenes expressing EGFP observed in our previous experiments (on average, 41% of transgenes selected at stage 46 reached stage 60; refs. 22,23 and unpublished observations). This indicates that Katushka, as well as EGFP, may exert lower toxic effect on living cells than other fluorescent proteins. Low toxicity of Katushka protein is also confirmed by the fact that six-month-old frogs developed from Katushka transgenic tadpoles, look absolutely normal, having body sizes similar to those of their nontransgenic siblings, which developed in parallel (data not shown).

Development of monomeric Katushka

Because Katushka is dimeric, as its parent protein, TurboRFP (**Supplementary Fig. 5** online), it can not be widely applied for labeling cellular proteins. Development of a monomeric variant of Katushka of similar spectral characteristics was therefore highly desirable.

Recently we have generated a monomeric red fluorescent version of TurboRFP, named TagRFP (excitation/emission peaks at 555/584 nm), which is characterized by high brightness, fast and complete chromophore maturation and high pH-stability. TagRFP has been shown to be an excellent monomeric red fluorescent label for protein tagging[17].

To exploit the monomeric properties of TagRFP, we mutated residues surrounding its chromophore to those of Katushka; these substitutions included R69K, N148S, F181L and H203R, among others. Of the variants generated, these four amino acid changes were necessary and sufficient to yield a normally maturing protein, named mKate, with spectral characteristics similar to those of Katushka (**Fig. 1b**,**c**).

Characterization of mKate

According to the gel-filtration data, mKate is monomeric at concentration as high as 10 mg/ml (**Supplementary Fig. 5**). The spectral characteristics of mKate are summarized in **Table 1**. Fluorescence spectra are almost identical to those of Katushka (**Fig. 1b**), with excitation and emission spectra peaking at 588 nm and 635 nm, respectively. The fluorescence quantum yield for mKate is 0.33, and the extinction coefficient is 45,000 M^{-1} cm^{-1}, resulting in a calculated brightness of 0.45 of EGFP (**Table 1**). mKate is characterized by complete and relatively fast chromophore maturation at 37 °C (half-time of 75 min). The pH-stability of mKate fluorescence is reasonable ($pK_a = 6.0$) but less than that of Katushka ($pK_a = 5.5$).

mKate formed no visible aggregates and did not localize nonspecifically when expressed alone either in HeLa or Phoenix Eco cells (**Supplementary Figs. 3** and **6** online). To verify the utility of mKate as a fusion tag, we fused it to β-actin and α-tubulin. The latter fusion strictly requires monomeric and nonaggregating fluorescent protein properties to allow successful tagging without aggregation and improper localization effects. Expression of both β-actin and α-tubulin fusions resulted in clear and accurate labeling of actin filaments and microtubules, respectively (**Supplementary Fig. 6**).

Comparison of photostability

Photostability is a key characteristic of a fluorescent dye, which determines its applicability for acquisition of high-resolution images and for monitoring in long time series in living cells and organisms. We compared photostability of Katushka and mKate in living HeLa cells with that of a number of widely used fluorescent proteins in two experimental systems: bleaching in a confocal microscope using appropriate laser line, and bleaching using a mercury arc lamp. Photobehavior and relative photostability of proteins depended on the light source (**Fig. 3** and **Table 2**). We presume that the key difference is that an arc lamp provides continuous irradiation, whereas confocal scanning implies short pixel dwelling time (the time the laser spends at every irradiated point).

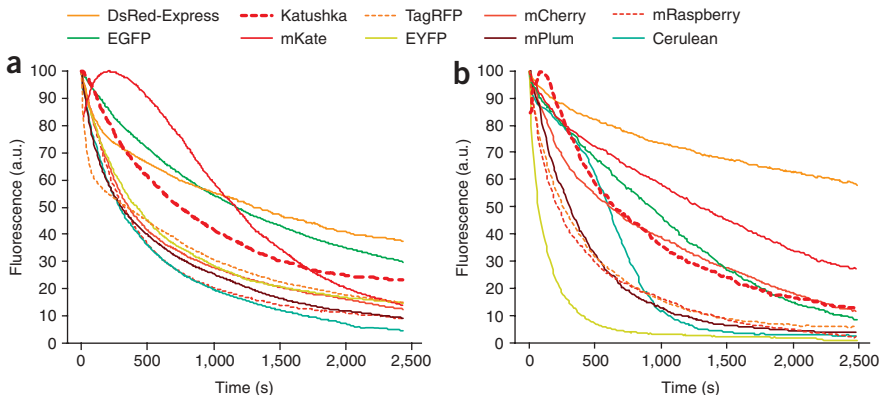

Figure 3 | Photobleaching experiments in living HeLa cells. (**a**) Leica SP2 confocal microscope, excitation by appropriate laser lines. (**b**) Leica AFLX 6000 fluorescent microscope, excitation by mercury arc lamp using an appropriate filter set.

Table 2 | Comparison of photostability for selected fluorescent proteins

Fluorescent protein	Excitation/ emission maxima (nm)	Laser line used (nm)	$t_{0.5}$ for bleach (s; laser line)	Excitation filter used (nm)	$t_{0.5}$ for bleach (s: arc lamp)
Cerulean	433/475	458	287	426–446	610
EGFP	484/510	488	1,167	450–490	910
EYFP	513/527	514	417	450–490	90
DsRed-Express	557/579	543	1,304	540–580	3,510
TagRFP	555/584	543	364	540–580	260
mCherry	587/610	543	352	540–580	630
mRaspberry	598/625	543	320	540–580	220
Katushka	588/635	543	745	540–580	700
mKate	588/635	543	1,154	540–580	1,260
mPlum	590/649	543	300	540–580	310

Katushka was characterized by relatively high photostability: the time to bleach 50% of fluorescence emission intensity in the confocal microscope was approximately twofold longer than that for EYFP (Clontech), mCherry[24], mPlum[15] or Cerulean[25] (**Fig. 3a** and **Table 2**). Upon arc-lamp irradiation (540–580 nm excitation filter, 200 mW/cm^2 output light power), Katushka demonstrated minor kindling-light growth of fluorescent signal within the first 90 s, followed by phobleaching kinetics close to that of mCherry (**Fig. 3b**). mKate demonstrated kindling-like activation in the confocal microscope only (**Fig. 3a**). The time to bleach 50% of mKate fluorescence was 3.6-fold and 5.7-fold longer compared to mRaspberry upon laser and arc-lamp irradiation, respectively (**Table 2**). Moreover, upon arc-lamp irradiation, mKate was the most stable among tested monomeric fluorescent proteins, being less stable than tetrameric DsRed-Express only (**Fig. 3b**).

Both Katushka and mKate demonstrated high photostability upon mercury arc lamp and laser light irradiation. But complex photobehavior of fluorescent proteins calls for additional studies, which should help to improve both fluorescent proteins themselves and microscopy techniques for their visualization.

DISCUSSION

Katushka combines far-red emission and brightness features of a fluorescent protein necessary for visualization within living tissues. Its excellent biochemical and spectral characteristics make it a powerful instrument for cancer research, developmental biology, gene expression and other whole-body imaging studies. Katushka's monomeric version, mKate, is preferable for protein labeling studies that require a monomeric far-red fluorescent tag.

The photobleaching measurements show that fluorescent proteins can exhibit complex photobehavior. Kindling-like photobehavior, as well as photobleaching effects, can distort quantitative analysis data and should be kept in mind when choosing fluorescent proteins and designing experiments. In contrast, kindling compensates for the photobleaching. For example, after 600 s of irradiation in a confocal microscope, the fluorescence brightness of mKate was approximately equal to its initial brightness. Our data indicate that different fluorescent proteins may be preferable for capturing single images and long time series. Indeed, although mKate was one of the most stable proteins to laser light within the first 1,000 s, the relatively low photostability of the second phase of photobleaching equalized the total photobleaching after 2,000 s of irradiation to that of mCherry and TagRFP (**Fig. 3a**).

Development of more red-shifted fluorescent proteins filling the gap between 650 and 700 nm of visible spectrum that are brighter and more photostable would raise sensitivity of the whole-body imaging techniques.

METHODS

Transgenic embryos. For transgenic experiments, we linearized vectors by *Sfi*I and purified them. We generated transgenic *X. laevis* embryos as previously described[22] and analyzed them using a Leica MZFLIII fluorescent stereomicroscope with the rhodamine filter set: excitation filter 546/10; suppression filter 565. To visualize a fluorescent signal emitted directly by internal embryonic tissues, we dissected the transgenic embryos using a microsurgical knife. The animal work was performed in Shemyakin and Ovchinnikov Institute of Bioorganic Chemistry, Russian Academy of Sciences, in accordance with the regulations of the Department of Health and Human Services, US National Institutes of Health.

Photobleaching experiments in living HeLa cells. Photobleaching by a laser line was performed on Leica SP2 confocal microscope, 63× oil immersion objective. Output power of laser lines was equalized (tuned to 40 μW in a parked laser mode). We used the following parameters: beam expander 1 (providing high intensity of excitation light), zoom 4×, scan frequency 400 Hz, format 512 × 512 pixels, 1 image per 1.63 s. Photobleaching by mercury arc lamp was performed on Leica AFLX 6000 fluorescent microscope, using an appropriate filter set and equalized output light power (approximately 200 mW/cm^2).

Additional Methods. Descriptions of cloning, gene construction and characterization of fluorescent proteins *in vitro* are available in **Supplementary Methods**.

Note: Supplementary information is available on the Nature Methods website.

ACKNOWLEDGMENTS

We thank N.E. Yelina (University of East Anglia, UK) for critical reading of the manuscript. Supported by grants from Howard Hughes Medical Institute 55005618, Molecular and Cell Biology, Russian Academy of Sciences, European Commission FP-6 Integrated Project LSHG-CT-2003-503259, Russian Foundation of Basic Research 07-04-12189 and the US National Institutes of Health GM070358. D.M.C. and K.A.L. are supported by Grant of the President of Russian Federation MK-8236.2006.4, and Russian Science Support Foundation. Partially supported by grants from Howard Hughes Medical Institute 55005630, MCB Russian Academy of Sciences, Russian Foundation of Basic Research 07-04-00466 and Civilian Research and Development Foundation RUB1-2826-MO-06 to A.G.Z.

AUTHOR CONTRIBUTIONS

D.S., E.M.M., T.V.C. and A.F.F. developed Katushka and mKate and characterized the proteins *in vitro* and in living cells. G.V.E., E.A.S. and A.G.Z. performed experiments with *X. laevis* and contributed to the writing of the manuscript. E.A.B., K.A.L., S.L. and D.M.C. designed and planned the project and wrote the manuscript.

COMPETING INTERESTS STATEMENT

The authors declare competing financial interests: details accompany the full-text HTML version of the paper at http://www.nature.com/naturemethods.

Published online at http://www.nature.com/naturemethods
Reprints and permissions information is available online at http://npg.nature.com/reprintsandpermissions

1. Chapman, S., Oparka, K.J. & Roberts, A.G. New tools for *in vivo* fluorescence tagging. *Curr. Opin. Plant Biol.* **8**, 565–573 (2005).
2. Chudakov, D.M., Lukyanov, S. & Lukyanov, K.A. Fluorescent proteins as a toolkit for *in vivo* imaging. *Trends Biotechnol.* **23**, 605–613 (2005).

3. Hoffman, R.M. Advantages of multi-color fluorescent proteins for whole-body and *in vivo* cellular imaging. *J. Biomed. Opt.* **10**, 41202 (2005).
4. Passamaneck, Y.J., Di Gregorio, A., Papaioannou, V.E. & Hadjantonakis, A.K. Live imaging of fluorescent proteins in chordate embryos: from ascidians to mice. *Microsc. Res. Tech.* **69**, 160–167 (2006).
5. Stewart, C.N., Jr. Go with the glow: fluorescent proteins to light transgenic organisms. *Trends Biotechnol.* **24**, 155–162 (2006).
6. Seitz, G. *et al.* Visualization of xenotransplanted human rhabdomyosarcoma after transfection with red fluorescent protein. *J. Pediatr. Surg.* **41**, 1369–1376 (2006).
7. Wacker, S.A., Oswald, F., Wiedenmann, J. & Knochel, W. A green to red photoconvertible protein as an analyzing tool for early vertebrate development. *Dev. Dyn.* **236**, 473–480 (2007).
8. Lukyanov, K.A., Chudakov, D.M., Lukyanov, S. & Verkhusha, V.V. Innovation: photoactivatable fluorescent proteins. *Nat. Rev. Mol. Cell. Biol.* **6**, 885–891 (2005).
9. Chudakov, D.M. *et al.* Kindling fluorescent proteins for precise *in vivo* photolabeling. *Nat. Biotechnol.* **21**, 191–194 (2003).
10. Stark, D.A. & Kulesa, P.M. An *in vivo* comparison of photoactivatable fluorescent proteins in an avian embryo model. *Dev. Dyn.* **236**, 1583–1594 (2007).
11. Bertera, S. *et al.* Body window-enabled *in vivo* multicolor imaging of transplanted mouse islets expressing an insulin-Timer fusion protein. *Biotechniques* **35**, 718–722 (2003).
12. Mirabella, R., Franken, C., van der Krogt, G.N., Bisseling, T. & Geurts, R. Use of the fluorescent timer DsRED-E5 as reporter to monitor dynamics of gene activity in plants. *Plant Physiol.* **135**, 1879–1887 (2004).
13. Konig, K. Multiphoton microscopy in life sciences. *J. Microsc.* **200**, 83–104 (2000).
14. Gurskaya, N.G. *et al.* GFP-like chromoproteins as a source of far-red fluorescent proteins. *FEBS Lett.* **507**, 16–20 (2001).
15. Wang, L., Jackson, W.C., Steinbach, P.A. & Tsien, R.Y. Evolution of new nonantibody proteins via iterative somatic hypermutation. *Proc. Natl. Acad. Sci. USA* **101**, 16745–16749 (2004).
16. Shkrob, M.A. *et al.* Far-red fluorescent proteins evolved from a blue chromoprotein from *Actinia equina*. *Biochem. J.* **392**, 649–654 (2005).
17. Merzlyak, E.M. *et al.* Bright monomeric red fluorescent protein with an extended fluorescence lifetime. *Nat. Methods* **4**, 555–557 (2007).
18. Petersen, J. *et al.* The 2.0-A crystal structure of eqFP611, a far red fluorescent protein from the sea anemone *Entacmaea quadricolor*. *J. Biol. Chem.* **278**, 44626–44631 (2003).
19. Wiedenmann, J. *et al.* Red fluorescent protein eqFP611 and its genetically engineered dimeric variants. *J. Biomed. Opt.* **10**, 14003 (2005).
20. Mohun, T.J., Garrett, N. & Gurdon, J.B. Upstream sequences required for tissue-specific activation of the cardiac actin gene in *Xenopus laevis* embryos. *EMBO J.* **5**, 3185–3193 (1986).
21. Nieuwkoop, P.D. & Faber, J. *Normal Table of Xenopus laevis* (*Daudin*). (Elsevier, Amsterdam, 1967).
22. Martynova, N. *et al.* Patterning the forebrain: FoxA4a/Pintallavis and Xvent2 determine the posterior limit of Xanf1 expression in the neural plate. *Development* **131**, 2329–2338 (2004).
23. Ermakova, G.V., Solovieva, E.A., Martynova, N.Y. & Zaraisky, A.G. The homeodomain factor Xanf represses expression of genes in the presumptive rostral forebrain that specify more caudal brain regions. *Dev. Biol.* **307**, 483–497 (2007).
24. Shaner, N.C. *et al.* Improved monomeric red, orange and yellow fluorescent proteins derived from *Discosoma* sp. red fluorescent protein. *Nat. Biotechnol.* **22**, 1567–1572 (2004).
25. Rizzo, M.A., Springer, G.H., Granada, B. & Piston, D.W. An improved cyan fluorescent protein variant useful for FRET. *Nat. Biotechnol.* **22**, 445–449 (2004).
26. Yanushevich, Y.G. *et al.* A strategy for the generation of nonaggregating mutants of *Anthozoa* fluorescent proteins. *FEBS Lett.* **511**, 11–14 (2002).
27. Terskikh, A.V., Fradkov, A.F., Zaraisky, A.G., Kajava, A.V. & Angres, B. Analysis of DsRed mutants Space around the fluorophore accelerates fluorescence development. *J. Biol. Chem.* **277**, 7633–7636 (2002).
28. Bevis, B.J. & Glick, B.S. Rapidly maturing variants of the *Discosoma* red fluorescent protein (DsRed). *Nat. Biotechnol.* **20**, 83–87 (2002).
29. Wiedenmann, J. *et al.* A far-red fluorescent protein with fast maturation and reduced oligomerization tendency from *Entacmaea quadricolor* (*Anthozoa, Actinaria*). *Proc. Natl. Acad. Sci. USA* **99**, 11646–11651 (2002).